Springer

KSME

Journal of Mechanical Science and Technology 32 (9) (2018) 4089~4101
www.springerlink.com/content/1738-494x(Print)/1976-3824(Online)
DOI 10.1007/s12206-018-0808-2

Reliability analysis of a nonlinear rotor/stator contact system in the presence of aleatory and epistemic uncertainty †

Lechang Yang[1,*], Ketai He[1] and Yanling Guo[2]

[1]*School of Mechanical Engineering, University of Science and Technology Beijing, Beijing 100083, China*
[2]*School of Automation Science and Electrical Engineering, Beihang University, Beijing 100191, China*

(Manuscript Received October 25, 2017; Revised March 20, 2018; Accepted May 10, 2018)

Abstract

On the basis of an overview of the global responses of a nonlinear Jeffcott rotor/stator contact model, the system reliability was evaluated subject to mixed aleatory-epistemic uncertainty. We used a likelihood-based approach for reliability modeling and analysis. In the context of uncertainty quantification, some advanced Bayesian techniques were adopted to reduce the computation cost in traditional Monte Carlo method. The parameters' effects on reliability were studied, incorporating both rotor physical background and inherent uncertain factors. This framework could be applied in the field of industrial manufacturing & mounting, risk assessment, product maintaining and benefit rotary machines from design phase to operation stage.

Keywords: Jeffcott rotor; Global response; Reliability analysis; Aleatory and epistemic uncertainty; Likelihood-based approach

1. Introduction

Motivated by the requirements in many mission-critical industries, e.g., infrastructure, aviation manufacturing and high-level national security, the design speed of rotary machinery keeps climbing. On the other hand, the clearance between rotor and stator is reduced to enhance the efficiency. In the context of operation safety, the rotor/stator unexpected rubbing may significantly degrade the machine performance, even leading to devastating consequences, which is not rare in practical engineering. The demand for reliability analysis for a rotating machine product in its design process is urgent.

Since Black [1] explored the dynamics of rub-related phenomena for rotor/stator contact systems in 1968, sufficient attention has been paid on the study of response of rotor/stator coupled system in deterministic scenario. Researchers try to capture its nonlinear nature through experimental investigations. A huge amount of rotor/stator dynamic behaviors with different features have been observed, such as the jump phenomenon and the synchronous full annular rubs [2-4], the partial rubs in sub- and super-synchronous whirl [5-7], the partial rubs in quasi-periodic whirl [8], the chaotic motion [9-11] as well as dry whip [12-14] for different parameter settings. Possessing the advantages of rapidly growing computer-aided techniques, it is desirable to discover the possible relationship between the multiple system responses and the specified parameters settings in an analytical way. Jiang et al. [15, 16] analytically derived an overall picture of the global response characteristics for a modified Jeffcott rotor, and the results are consistent with the experiment mentioned above.

Getting deep insights into practical engineering, the various uncertain factors induced in design process or in manufacturing stage are inevitable, and their influence on system response should not be overlooked. This problem has been realized in recent years and addressed in a series of publications [17-19]. These research works have made profound contributions to the rotor-related research field considering parameter uncertainty [20-23]. However, most of these works only focus on the study of mathematical representations of uncertain parameters (probability & fuzzy [24-26], fuzzy & interval [27], probability & interval [28-30]) while paying less attention to its further application to reliability engineering. Limited exceptions are the works from Refs. [31-35]. Not many examples can be found in the field of reliability engineering for rotor/stator contact system subject to mixed aleatory-epistemic uncertainty. The issue of reliability analysis for a nonlinear rotor/stator coupled system has not been sufficiently addressed yet.

To fill the research gap and establish a more generic framework, we tried to obtain a global reliability analysis result of a Jeffcott rotor/stator contact model in an analytical way, which serves as a simplified model for most engineering rotor devices. Special attention has been paid to the reliability criteria

*Corresponding author. Tel.: +86 10 6233 3868
E-mail address: yanglechang@126.com
† Recommended by Associate Editor Byeng Dong Youn

for nonlinear systems, and a novel statistical method is adopted to deal with the possible mixed uncertainty in practical engineering.

This paper is organized as follows. The physical model of the selected rotor/stator contact system and its governing equations are presented in Sec. 2, along with the analyses of system response under ideal circumstance (deterministic) in Sec. 3. Sec. 4 illustrates the adopted reliability techniques and some notations of the proposed approach. The effects of parameters on system reliability are particularly focused in Sec. 5. Sec. 6 discusses the benefits of this work and some notes. Finally, some concluding remarks are drawn in Sec. 7.

2. Rotor-stator contact model and governing equation

We examined a typical Jeffcott rotor-stator coupled system, which consists of an eccentric rotor and a rigidly fixed stator with elastic surface (see Fig. 1). The stator, which is rigidly fixed, has an elastic contact surface and is modeled as the radial springs with stiffness k_s. The rotor, which is divided into a massless shaft with stiffness k_r and a disk with mass m, rotates inside the stator at speed ω. Subject to out-of-balance mass, the rotor may make intermittent contacts with the stator during operation, resulting in complex dynamic behavior. Given the rotor eccentricity e, external damping c , friction coefficient f_c and gap between rotor and stator r_0, the motion equation is expressed as Eq. (1), neglecting the stator inertia and gyroscopic effect.

The motion equation is given as

$$\begin{cases} m\ddot{x}+c\dot{x}+k_r x+\theta k_s\left(1-\dfrac{r_0}{r}\right)\left(x-sign\left(v_{rel}\right)f_c y\right) \\ =me\omega^2\cos\omega t \\ m\ddot{y}+c\dot{y}+k_r y+\theta k_s\left(1-\dfrac{r_0}{r}\right)\left(sign\left(v_{rel}\right)f_c x+y\right) \\ =me\omega^2\sin\omega t \end{cases}, \quad (1)$$

$$\theta=\begin{cases}0, \sqrt{x^2+y^2}<r_0\\ 1, \sqrt{x^2+y^2}>r_0\end{cases}$$

where the v_{rel} represents the relative velocity between the rotor and stator at the contact point, indicating the sign function $sign\left(v_{rel}\right)=1$ when the rotor whirls forward, otherwise, $sign\left(v_{rel}\right)=-1$. For mathematical convenience, it could be rewritten in matrix form as

$$\mathbf{m}\ddot{\mathbf{q}}+\mathbf{c}\dot{\mathbf{q}}+\left(\mathbf{k}_\mathbf{r}+sign\left(r\right)\cdot\mathbf{k}_\mathbf{s}\right)\mathbf{q}=\mathbf{f}\left(\mathbf{t}\right) \quad (2)$$

where

$$\mathbf{q}=\begin{bmatrix}x\\y\end{bmatrix},\mathbf{m}=\begin{bmatrix}m&0\\0&m\end{bmatrix},\mathbf{c}=\begin{bmatrix}c&0\\0&c\end{bmatrix},\mathbf{k}_\mathbf{r}=\begin{bmatrix}k_r&0\\0&k_r\end{bmatrix},$$

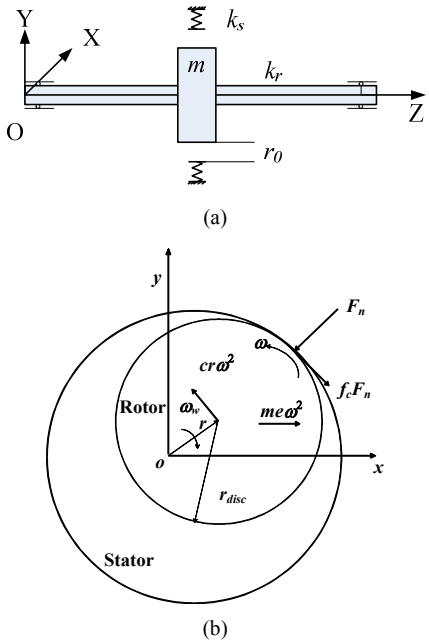

Fig. 1. (a) Schematic diagram of the rotor/stator system; (b) applied forces of rotor during whirling.

$$sign\left(r\right)=\begin{cases}0, \sqrt{x^2+y^2}<r_0\\ 1, \sqrt{x^2+y^2}>r_0\end{cases},\mathbf{f}\left(\mathbf{t}\right)=me\omega^2\begin{bmatrix}\cos\omega t\\ \sin\omega t\end{bmatrix},$$

$$\mathbf{k}_\mathbf{s}=k_s\left(1-\frac{r_0}{r}\right)\begin{bmatrix}1&-sign\left(v_{rel}\right)f_c\\ sign\left(v_{rel}\right)f_c&1\end{bmatrix}.$$

Through a non-dimensional transformation, Eq. (2) is reformulated as

$$\ddot{\mathbf{Q}}+\mathbf{Z}\dot{\mathbf{Q}}+\left(\mathbf{B}+sign\left(R\right)\cdot\mathbf{K}_s\right)\mathbf{Q}=\mathbf{F}\left(\mathbf{t}\right) \quad (3)$$

where

$$\mathbf{Q}=\begin{bmatrix}X\\Y\end{bmatrix},\mathbf{Z}=\begin{bmatrix}2\zeta&\\&2\zeta\end{bmatrix},\mathbf{B}=\begin{bmatrix}\beta&\\&\beta\end{bmatrix},$$

$$sign\left(R\right)=\begin{cases}0, \sqrt{X^2+Y^2}<R_0\\ 1, \sqrt{X^2+Y^2}>R_0\end{cases},\mathbf{F}\left(\mathbf{t}\right)=\Omega^2\begin{bmatrix}\cos\Omega\tau\\ \sin\Omega\tau\end{bmatrix}$$

$$\mathbf{K}_\mathbf{s}=\left(1-\frac{R_0}{R}\right)\begin{bmatrix}1&-sign\left(V_{rel}\right)f_c\\ sign\left(V_{rel}\right)f_c&1\end{bmatrix}.$$

The non-dimensional variables are defined as

$$X=\frac{x}{e},Y=\frac{y}{e},R_0=\frac{r_0}{e},R=\frac{r}{e},2\zeta=\frac{c}{\sqrt{mk_s}},$$

$$\Omega=\frac{\omega}{\omega_2},\beta=\frac{k_r}{k_s},\omega_2^2=\frac{k_s}{m},\tau=\omega_2 t$$

where ω_2 is the natural frequency of the elastic contact surface.

Eq. (3) is piecewise smooth depending on the value of outer sign function $sign(R)$ and inner sign function $sign(V_{rel})$. Note that a new time scale $\tau = \omega_2 t$ was introduced and the differentiation in Eq. (3) is with respect to the new time variable τ.

3. Deterministic system response and stability analysis

There are multi-types of system responses, which are governed by different phase of the piecewise smooth equation. Since our goal was to assess the system reliability on whole parameter plane and determine the safe domain for rotor proper operation, it is desirable to derive an overview picture of the system global response analytically.

3.1 No-rub synchronous motion

The periodic solution of Eq. (3) has the following general form

$$\mathbf{Q} = \begin{bmatrix} X \\ Y \end{bmatrix} = \begin{bmatrix} R\cos(\Omega\tau + \psi) \\ R\sin(\Omega\tau + \psi) \end{bmatrix}. \tag{4}$$

If the gap between rotor and stator is less than initial clearance, no contact occurs: $sign(R) = 0$. Thus, the governing equation is simplified to be linear; the amplitude and phase angle can be obtained by substituting Eq. (4) into Eq. (3) as

$$R = \frac{\Omega^2}{\sqrt{\left(\beta - \Omega^2\right)^2 + 4\zeta^2\Omega^2}}, \tan\psi = \frac{2\zeta\Omega}{\Omega^2 - \beta}. \tag{5}$$

This solution is only physically valid when the steady amplitude R is less than clearance R_0. Let $R \le R_0$, the parameter boundary condition for no-rub synchronous solution is derived as Eq. (6).

$$\left(R_0^2 - 1\right)\Omega^4 + R_0^2\left(4\zeta^2 - 2\beta\right)\Omega^2 - 4R_0^2\zeta\Omega + R_0^2\beta^2 \ge 0. \tag{6}$$

Since the solution is always stable for a linear case, the two real roots Ω_l and Ω_u, solved from Eq. (6), can be used to determine the parameter boundary of no-rub motion.

3.2 Synchronous full annular rub

However, as the rotation speed keeps increasing, the time-varying gap will exceed a threshold, leading continuous rubbing. The rotor gets engaged with the stator, and the motion equation becomes nonlinear. In this circumstance, the rotor-stator coupled system exhibits complex dynamic behavior. For nonlinear scenario ($sign(R) = 1$), after substituting Eq. (4) into Eq. (3) and some simplification, we have

$$\begin{aligned} &(-R\Omega^2 + \beta R + R - R_0)\cos(\Omega\tau + \psi) + \\ &(-2\zeta R\Omega - f_c R + f_c R_0)\sin(\Omega\tau + \psi) = \Omega^2\cos\Omega\tau. \end{aligned} \tag{7}$$

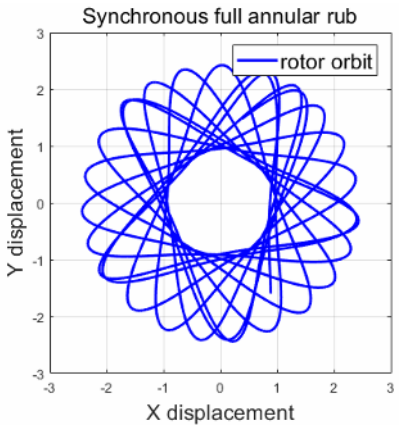

Fig. 2. Rotor orbit for typical synchronous full annular rub.

Noting that Eq. (7) is valid for all non-dimensional time variable τ, let $\Omega\tau + \psi = 0$ and $\Omega\tau + \psi = \pi/2$ respectively, so we have

$$\begin{aligned} &-2\zeta R\Omega - f_c R + f_c R_0 - \Omega^2\sin\psi = 0 \\ &-R\Omega^2 + \beta R + R - R_0 - \Omega^2\cos\psi = 0. \end{aligned} \tag{8}$$

Using mathematical transformation to eliminate phase angle ψ, a polynomial about amplitude R is derived.

$$a_2 R^2 + a_1 R + a_0 = 0 \tag{9}$$

where

$$\begin{aligned} a_2 &= \left(2\zeta\Omega + f_c\right)^2 + \left(1 + \beta - \Omega^2\right)^2 \\ a_1 &= -2R_0\left[\left(1 + \beta - \Omega^2\right) + f_c\left(2\zeta\Omega + f_c\right)\right] \\ a_0 &= R_0^2\left(1 + f_c^2\right) - \Omega^4. \end{aligned}$$

Since only the steady-state periodic solution is of interest, we differentiate Eq. (9) with respect to amplitude R, and set $dR_0/R = 0$. It is derived as $a_1^2 - 4a_0a_2 = 0$, namely,

$$\begin{aligned} &\Omega^2\left(\Omega^2 + 4\zeta^2 - 2\right) + \left(1 + \beta\right)^2 + f_c^2 \\ &+\left(\Omega^2 - f_c^2 - 1 - \beta\right)R_0/R = 0. \end{aligned} \tag{10}$$

Eq. (10) is the so-called saddle-node bifurcation condition (or turning point), while the nonlinear solutions are called full annular rub solutions, when the amplitudes satisfy $R > R_0$. Fig. 2 shows a typical rotor orbit for synchronous full annular rub solution of the rotor-stator coupled system. The schematic diagram of applied force analysis is referred to for better understanding.

3.3 Quasi-period partial rub

Quasi-periodic partial rub is a type of response that the rotor contacts the stator intermittently. For the partial rub, both lin-

ear and nonlinear equations should be considered. Since the synchronous full annular rub bifurcates into partial rub through Hopf bifurcation, the Hopf bifurcation condition serves as the boundary between synchronous full annular rub and partial rub.

According to the Hopf bifurcation theory, there should be one pair of conjugate purely imaginary eigenvalues for the Jacobian matrix. By substituting $\lambda = i\omega$ (or $\lambda = -i\omega$) into the characteristic equation Eq. (11)

$$\lambda^4 + b_3\lambda^3 + b_2\lambda^2 + b_1\lambda + b_0 = 0 \tag{11}$$

where the coefficients b_0~b_3 are given as

$$\begin{aligned} b_3 &= 4\zeta \\ b_2 &= 4\zeta^2 + 2\Omega^2 + 2(1+\beta) - R_0/R \\ b_1 &= 4\left(f_c\Omega + \zeta + \beta\zeta + \Omega^2\zeta\right) - 2\left(f_c\Omega + \zeta\right)R_0/R \\ b_0 &= \Omega^2\left(\Omega^2 + 4\zeta^2 - 2\right) + \left(1+\beta\right)^2 + f_c^2 + \left(\Omega^2 - f_c^2 - 1 - \beta\right)R_0/R . \end{aligned}$$

Eq. (12) is derived as

$$b_1^2 - b_1 b_2 b_3 + b_0 b_3^2 = 0, \quad b_1 b_3 > 0 . \tag{12}$$

Rewriting Eq. (12) in a polynomial of amplitude R as

$$c_2 R^2 + c_1 R + c_0 = 0 \tag{13}$$

where the coefficients c_0~c_2 are given as

$$\begin{aligned} c_2 &= 16\left[4\zeta^2(1+\beta) - f_c^2\right]\left(\zeta^2 + \Omega^2\right) \\ c_1 &= 16R_0\left(f_c\beta - 2\zeta^2\right)\left(\Omega^2 + \zeta^2\right) \\ c_0 &= 4R_0^2\left(\zeta^2 - f_c^2\Omega^2\right) . \end{aligned}$$

After eliminating R, a twelve-order polynomial of rotation speed Ω is also obtained and the boundary of Hopf bifurcation can be numerically solved. Fig. 3 shows a typical rotor orbit for quasi-periodic partial rub solution of the rotor-stator coupled system.

4. Reliability analysis subjected to mixed aleatory-epistemic uncertainties

In the previous section, the multiple responses of a rotor/stator contact system were analytically investigated for deterministic scenario. However, in practical engineering, a huge amount of uncertain factors will be introduced in the phase of design, manufacturing, mounting etc. Addressing its reliability, a likelihood-based uncertainty quantification approach is proposed, which enables the reliability analysis to perform in the context of mixed aleatory-epistemic uncertainties.

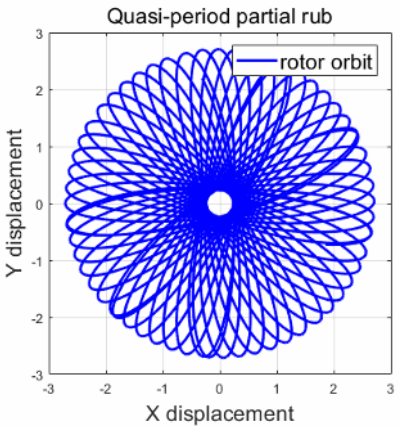

Fig. 3. Rotor orbit for typical quasi-period partial rub.

4.1 Notation

4.1.1 Mixed aleatory-epistemic uncertainty

According to the well-accepted uncertainty theory [36, 37], the various uncertainties (model uncertainty, parameter uncertainty etc.) in practice can be classified into aleatory uncertainty and epistemic uncertainty from a mathematical perspective.

Aleatory uncertainty comes from the stochastic nature of one problem and is usually thought to be irreducible. Epistemic uncertainty is induced either by a lack of knowledge or a bias of existing judgment, which can be reduced when new information becomes available. Aleatory uncertainty is usually represented in the probability distribution form, while epistemic uncertainty has more complicated mathematical forms, such as interval variable or a coexistence of probability and interval. In this study, we considered both aleatory and epistemic uncertainties.

4.1.2 Reliability

Reliability is defined as the probability that one device will perform its intended function within a specified period of time (the time before system response exceeds a predefined threshold). It can be calculated as the integration of the joint probability density function (PDF) over the entire safe region as Eq. (14)

$$R(t) = \Pr(Z > 0) = \int_{Z>0} f(Z)dZ \tag{14}$$

where Z denotes the random system response of interest, and $f(Z)$ corresponds to the joint PDF of random variable Z.

For the specified rotor/stator contact system, if the clearance between rotor and stator is used to build state function, the limit state function can be generally presented as

$$Z = g(\Omega, f_c, R_0, \beta, \zeta) = R - R_0 . \tag{15}$$

When the clearance is less than the initial clearance R_0, the

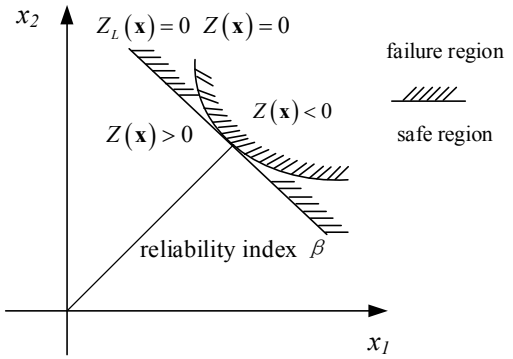

Fig. 4. The limit state function and corresponding safe region (failure region).

rotor will not contact with the stator, and the device is assumed to be working normally. However, if the clearance is greater than R_0, the rotor will get engaged with the stator. In certain circumstance, the rotor may rub the stator surface heavily, which leads to a catastrophic failure of the whole machine. These two scenarios can be simply expressed as Eq. (16) and intuitively shown in Fig. 4.

$$\begin{cases} Z = g(\Omega, f_c, R_0, \beta, \zeta) > 0, & safe \quad state \\ Z = g(\Omega, f_c, R_0, \beta, \zeta) < 0, & failure \quad state . \end{cases} \tag{16}$$

The challenges that we are facing are twofold: First, the traditional reliability theory is constructed in the field of probability; thus a comprehensive reliability analysis is hard to perform, taking mixed uncertainty (including sparse data point and interval variable) into consideration. Secondly, due to its strong nonlinearity, the reliability criteria are not simple and clear since there may be multiple steady system responses coexisting (e.g. a coexistence of no-rub synchronous motion and full annular rub).

We deal with the first issue by adopting a likelihood-based uncertainty quantification approach, which enables the reliability analysis to be performed in a unified way. The second issue will be discussed in Sec. 5, since the criteria should be case-based determined.

4.2 Likelihood-based uncertainty quantification approach

4.2.1 Construction likelihood for non-probabilistic information

Consider a stochastic variable X that follows one specific distribution (e.g. Normal) with a series of sparse data, and its probability density function (PDF) is denoted as $p(x|\Theta)$ where Θ is the parameter set. The likelihood function $L(\Theta|x)$ is defined as the probability of the observation of given data set, which is conditioned on the distribution parameter Θ. Strictly speaking, the probability value for any discrete point data is zero for a continuous density function, so the likelihood function is derived by considering the probability of an infinitesimally small interval around x_i on the basis of the mean value theorem as Eq. (17) for practical use.

$$\begin{aligned} L(\Theta) &\propto P\left(X \in \left(x_i - \frac{\varepsilon}{2}, x_i + \frac{\varepsilon}{2}\right) | \Theta\right) \\ &= \int_{x_i-\varepsilon/2}^{x_i+\varepsilon/2} p_X(x|\Theta)dx = \varepsilon\, p_X(x_i|\Theta) \propto p_X(x_i|\Theta). \end{aligned} \tag{17}$$

A similar idea can be extended to bounded interval dat; thus the expression for likelihood of the parameters Θ for interval $[a, b]$ is

$$\begin{aligned} L(\Theta) &\propto P(a \le x \le b | \Theta) \\ &= \int_a^b p_X(x|\Theta)dx = F_X(b|\Theta) - F_X(a|\Theta). \end{aligned} \tag{18}$$

It is the cumulative density function (CDF) $F_X(\ )$ rather than PDF $p_X(\ )$ that would be used. For multiple input interval information, the combined likelihood function is expressed as

$$L(\Theta) \propto \left[\prod_{i=1}^{n}\left[F_X(b_i|\Theta) - F_X(a_i|\Theta)\right]\right]. \tag{19}$$

4.2.2 Representation of epistemic uncertainty with pure interval data

This subsection presents an approach to deal with pure interval uncertainty. To begin with, a sole interval $[a, b]$ is assigned to the uncertain variable X, namely, $X \in [a,b]$. From the probabilistic perspective, it can be interpreted as $X \sim U(a,b)$ since the chance that variable X takes any value within the range of $[a, b]$ is equal. It can be interpreted as an optimization problem as follows:

Object: $f(x)$

Subject: (1) $f(x) \ge 0$ (2) $\int_a^b f(x)dx = 1$ (3) $f(x) \equiv p$.

The solved PDF $f(x)$ is the corresponding probabilistic description for the given interval $[a, b]$.

There may be multiple interval information available for a specified variable X in practical engineering, which occurs when information are collected from different (independent) sources, (e.g., judgments from expert system). To deal with this, the principle above is extended to multiple intervals. For N input intervals $x \in [a_i, b_i], 1 \le i \le N$, there are total *2N-1* subintervals $[d_j, d_{j+1}], a_{\min} \le d_j \le d_{j+1} \le b_{\max}$, where a_{min} is the lower bound and b_{max} is the upper bound, respectively. The corresponding optimization problem is transformed as

Object: $f(x)$

Subject: (1) $f(x) \ge 0$ (2) $\int_a^b f(x)dx = 1$

(3) $\dfrac{f(x_1)}{f(x_2)} = \dfrac{M(x_1)}{M(x_2)}, \forall x_1, x_2 \in [a_{\min}, b_{\max}]$

Table 1. Algorithm for representation of pure interval uncertainty.

Calculate the basic weight as $\Delta = 1 \Big/ \sum_{i=1}^{N} \left(b_i - a_i\right)$
Count if $x \in \left[a_i, b_i\right]$, for $x \in \left[a_{\min}, b_{\max}\right]$ $i = 1:N$
Compute the piecewise function $M\left(x\right)$
Construct the converted PDF as $f_j\left(x\right) = \Delta \cdot M_j\left(x\right), x \in \left[a_{\min}, b_{\max}\right], 1 \le j \le 2N-1$

where subject (1) and (2) come from the probability axiom and (3) is an additional constraint that makes the generated probability distribution proportional to the given multi-intervals. To balance the contribution of each interval, a mass function $M(x)$ is assigned. To analytically solve this optimization problem, the main steps of the developed algorithm are presented in Table 1.

Note that the constructed PDF is a *2N-1* piecewise function and usually cannot be expressed in parametric form.

4.2.3 Representation of epistemic uncertainty with additional probabilistic information

We discuss next the uncertainty quantification method when both interval and probabilistic information are available: A scenario with mixed uncertainties. This situation comes true when knowledge is obtained through different means. For instance, the rotor eccentricity e for a batch of rotary machine may be estimated by a series of intervals based on expert judgment. On the other hand, considering the design and manufacturing process, the source of uncertainty in eccentricity e is understood as the error/deviation accumulated during the procedure of assembling, mounting, etc., which generally follows the normal distribution.

If variable X is supposed to follow one specific distribution, the combined likelihood function can be expressed as Eq. (20). The distribution parameter Θ can be evaluated by maximizing the right hand side of Eq. (20) (popularly known as the *maximum likelihood estimate*, MLE). However, this calculation may be cumbersome because the cumulative density function of variable X is not always in analytical form (e.g., the CDF of normal distribution). Instead of computing statistics parameter Θ by maximizing the likelihood, we adopted some Bayesian-based techniques to estimate the *full likelihood*. Barnard et al. [38] emphasized the idea that the entire likelihood function should be used for inference rather than merely its maximization.

$$L\left(\Theta\right) \propto \left[\prod_{i=1}^{n}\left[f_X\left(x_i \mid \Theta\right)\right]\right] \left[\prod_{i=1}^{n}\left[F_X\left(b_i \mid \Theta\right) - F_X\left(a_i \mid \Theta\right)\right]\right]. \tag{20}$$

Assigning an appropriate prior distribution, the parameter Θ is estimated as Eq. (21) by adopting Bayesian rule

Table 2. Traditional double loop Monte Carlo method.

Suppose the model output $\boldsymbol{Y}$ is given by a deterministic function of $\boldsymbol{Y}=f(\boldsymbol{X})$
To get an estimated result of $\boldsymbol{Y}$:
Outer loop:
M samples of parameter $\boldsymbol{\theta}$ are generated from $p(\theta)$
Inner loop:
For a given θ
N samples of $\boldsymbol{X}$ generated from $p(X\|\theta)$
End loop
Output $\boldsymbol{Y}$ is calculated as $\boldsymbol{Y}=f(\boldsymbol{X})$ for a family of distributions of variable $\boldsymbol{X}$
End loop
The PDF of model output Y is estimated based on the $M \times N$ samples (such as kernel density estimate)

$$p\left(\boldsymbol{\Theta} \mid D\right) = \frac{l\left(\boldsymbol{\Theta} \mid D\right)\pi\left(\boldsymbol{\Theta}\right)}{\int l\left(\boldsymbol{\Theta} \mid D\right)\pi\left(\boldsymbol{\Theta}\right)d\boldsymbol{\Theta}} \tag{21}$$

where $\pi(\Theta)$ denotes the joint prior distribution of parameter vector Θ, while $p\left(\boldsymbol{\Theta} \mid D\right)$ is the estimated probability distribution of Θ. $l\left(\boldsymbol{\Theta} \mid D\right)$ is the combined likelihood function which has the same form as Eq. (20).

The parameter Θ estimated with the Bayesian method is a probability distribution, compared with a deterministic value by MLE method. Hence, a family of conditioned probability distributions for X is derived due to the uncertainty within the statistics parameter θ. A double loop Monte Carlo (or called as second-order Monte Carlo) method (Table 2) can be adopted for analysis, but this method may not be affordable for some complicated cases. To illustrate, suppose M samples of θ are generated in the outer loop, each of which corresponds to a distribution of $p(\theta)$, and N samples of X are drawn for each sample θ in the inner loop, and the computation cost is total $M \times N$. To get a satisfactory result, 10^4 samples are usually required for M and N; thus the number of total samples is too large for a general routine program.

Considering this, we discard the double loop sampling approach and construct the PDF of variable X as Eq. (22) to replace the family of distribution for $p\left(X \mid \theta\right)$ with a unique distribution $p\left(X\right)$

$$p\left(X\right) = \int p\left(X \mid \boldsymbol{\Theta}\right)p\left(\boldsymbol{\Theta}\right)d\boldsymbol{\Theta}\,. \tag{22}$$

The unconditional PDF $p\left(X\right)$ can be calculated by integrating the conditional PDF $p\left(X \mid \boldsymbol{\Theta}\right)$ over the entire parameter space of Θ.

4.3 Reliability method

The aforementioned likelihood-based approach was adopted to deal with the mixed aleatory-epistemic uncertainty, by which all non-probabilistic information is incorporated in a unified way; thus the reliability analysis is able to be performed. In Refs. [31, 32], the reliability of a rotor/stator sys-

Table 3. Available information and data collection for case study.

	Uncertainty	Available information	
Rotation speed Ω	Aleatory	Complete probability distribution	$\Omega \sim N(\mu_\Omega, \sigma_\Omega)$
Friction coefficient f_c	Epistemic	Multiple input intervals	Source 1 : $[0.05, 0.1]$, Source 2: $[0.1, 0.15]$ Source 3 $[0.15, 0.2]$, Source 4: $[0.2, 0.3]$
Clearance R_0	Epistemic	Probability distribution with uncertainty parameters and Multiple input intervals	$R_0 \sim N(\mu_{R_0}, \sigma_{R_0})$ Source 1 : $[1.5, 1.8]$ Source 2: $[2, 2.2]$ Source 3 $[1.7, 2.1]$ sparse point data: 1.75, 1.89, 2.13

tem is examined by applying a statistical fourth moment method, but the physical model is not sufficiently addressed. From an engineering perspective, it is of interest the fluctuation of reliability surface and the safe domain in parameter space rather than a reliability calculation result of certain parameter combinations. So we transform the concerned reliability problem into the following optimization problem and employ a second moment method substituting for the fourth moment method.

$$\text{Object:} \quad \min \beta = \|\mathbf{y}\| = \sqrt{\mathbf{y}^{\mathrm{T}}\mathbf{y}} = \sqrt{\sum_{i=1}^{n}\left(\frac{x_i - \mu_{X_i}}{\sigma_{X_i}}\right)^2}$$

$$\text{Subject:} \quad g_X(x_1, x_2, ..., x_n) = 0$$

where $g_X(x_1, x_2, ..., x_n)$ is the limit state function which is determined by a specified rotor/stator system. β is the so-called reliability index, and it has a one-to-one mapping relationship with the reliability (probability). The limit state function in Eq. (15) can be approximated by its first-order Taylor series at mean value point as

$$Z \approx Z_L = g_X(X^*) + \sum_{i=1}^{n}\frac{\partial g_X(x^*)}{\partial X_i}(X_i - x_i^*) + ... \tag{23}$$

And the reliability index β can be calculated as Eq. (24) taking the geometric interpretation of β into account (the reliability index β could be interpreted as the distance from coordinate origin to limit state surface, see in Fig. 4), if the basic variables are both normally distributed.

$$\beta = \frac{\mu_{Z_L}}{\sigma_{Z_L}} = \frac{g_X(x^*) + \sum_{i=1}^{n}\frac{\partial g_X(x^*)}{\partial X_i}(\mu_{X_i} - x_i^*)}{\sqrt{\sum_{i=1}^{n}\left[\frac{\partial g_X(x^*)}{\partial X_i}\right]^2 \sigma_{X_i}^2}} \tag{24}$$

where the first and second moment of Z_l are expressed as

$$\mu_{Z_L} = g_X(x^*) + \sum_{i=1}^{n}\frac{\partial g_X(x^*)}{\partial X_i}(\mu_{X_i} - x_i^*),$$

$$\sigma_{Z_L} = \sqrt{\sum_{i=1}^{n}\left[\frac{\partial g_X(x^*)}{\partial X_i}\right]^2 \sigma_{X_i}^2}.$$

Here x^* is the so-called expansion point, which satisfies the constraint of limit state function, namely, $g_X(x_1, x_2, ..., x_n) = 0$.

Eq. (24) is only valid when the basic variables follow normal distribution. Considering the possible situation with mixed aleatory-epistemic uncertainty, if the basic random variables in vector X^* are given as interval data or through a collection of samples, Eq. (24) is not able to be directly applied. To deal with this, the transformation of non-probabilistic into probability distribution has been discussed in a previous subsection, and for a series of discrete points, the kernel density estimator (KDE) was adopted to visualize the resulting distributions and to facilitate the computation of the reliability. A KDE is an approximation to the probability density function (PDF) of a source of values; it is computed based on *n* data points.

To establish a normal distribution, the Gaussian kernel is used and has the following form:

$$\hat{f}_s(s) = \frac{1}{n}\sum_{i=1}^{n}\frac{1}{\sqrt{2\pi}\varepsilon}\exp\left[-\frac{1}{2\varepsilon^2}(s - s_i)^2\right]. \tag{25}$$

Thus the probabilistic characterization of S is an approximation to its PDF that uses the kernel density estimator (KDE).

As the index β is determined, the probability of failure and reliability is therefore calculated as Eq. (26), respectively.

$$\begin{cases} P_f = \Phi(-\beta) \\ R = \Phi(\beta) \end{cases} \tag{26}$$

where Φ is the CDF of a standard normal distribution.

5. Reliability of nonlinear rotor/stator contact system

5.1 Mixed aleatory-epistemic uncertainty quantification

To illustrate and verify the mixed uncertainty quantification method proposed above, the likelihood-based approach is applied to rotor/stator contact system with governing equation of Eq. (3). We consider the uncertainty in three parameters (Ω, f_c, R_0) by setting other parameters as fixed value ($\zeta = 0.05$, $\beta = 0.04$). Specially, the rotation speed is set as a random variable, which follows a normal distribution as

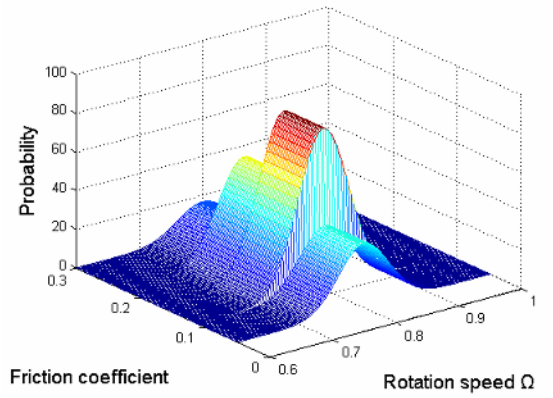

Fig. 5. Transformed joint PDF in Ω - f_c parameter plane.

$\Omega \sim N(\mu_\Omega, \sigma_\Omega)$, while the available information for clearance R_0 and friction coefficient f_c are given in mixed sparse-data and interval form as Table 3 shows.

The rotation speed Ω is given in a stochastic form, so there is no need for further transformation. For the friction coefficient f_c, it is the case of multiple input intervals without probabilistic information, and the algorithm in Table 1 is adopted to build the transformed PDF.

The converted PDF is constructed as

$$p = \begin{cases} 10/3 & f \in [0.05, 0.1] \\ 25/3 & f \in [0.1, 0.15] \\ 5 & f \in [0.15, 0.2] \\ 5/3 & f \in [0.2, 0.3] \end{cases}.$$

The joint PDF is constructed as Eq. (27) and shown in Fig. 5, since the rotation speed and friction coefficient are assumed to be independent.

$$p(\Omega, f_c \mid \Theta) = p(\Omega \mid \Theta)\, p(f_c \mid \Theta). \tag{27}$$

The clearance R_0, is assumed to follow a normal distribution, but the statistic parameters (μ and σ) are unknown. The available interval and sparse data are used to evaluate unknown distribution parameters. By adopting Bayesian rule, the likelihood of unknown parameters μ and σ is constructed as Eq. (28)

$$L(\boldsymbol{\Theta}) \propto \left[\prod_{i=1}^{m} f_X(x_i \mid \boldsymbol{\Theta})\right]\left[\prod_{i=1}^{n}\left[F_X(b_i \mid \boldsymbol{\Theta}) - F_X(a_i \mid \boldsymbol{\Theta})\right]\right] \tag{28}$$

where $f_X(\cdot)$ and $F_X(\cdot)$ denote the PDF and CDF of normal distribution respectively. $\boldsymbol{\Theta}$ is the parameter vector, and for this case $\boldsymbol{\Theta} = (\mu, \sigma), m = n = 3$.

Since there is no additional available information, the non-informative prior is assigned as $\mu \sim Uniform(a_\mu, b_\mu)$, $\sigma \sim Uniform(a_\sigma, b_\sigma)$. Thus prior $\pi(\boldsymbol{\Theta})$ can be taken out of integration and the posterior joint PDF is reduced to

$$p(\boldsymbol{\Theta} \mid D) = \frac{L(\boldsymbol{\Theta})\pi(\boldsymbol{\Theta})}{\int L(\boldsymbol{\Theta})\pi(\boldsymbol{\Theta})} = \frac{\left[\prod_{i=1}^{m} f_X(x_i \mid \boldsymbol{\Theta})\right]\left[\prod_{i=1}^{n}\left[F_X(b_i \mid \boldsymbol{\Theta}) - F_X(a_i \mid \boldsymbol{\Theta})\right]\right]}{\int\left[\prod_{i=1}^{m} f_X(x_i \mid \boldsymbol{\Theta})\right]\left[\prod_{i=1}^{n}\left[F_X(b_i \mid \boldsymbol{\Theta}) - F_X(a_i \mid \boldsymbol{\Theta})\right]\right] d\boldsymbol{\Theta}}. \tag{29}$$

There is usually no analytical solution for Eq. (29), so the posterior joint PDF is numerically solved. The marginal distributions of the parameter μ and σ are depicted in Figs. 6(a) and (b).

The unconditional PDF is obtained by integrating over the space of parameters $\boldsymbol{\Theta}$ as

$$p(R_0 \mid data) = \int p(R_0 \mid \Theta) p(\Theta \mid data)\, d\Theta. \tag{30}$$

Fig. 6(c) presents the unconditioned posterior PDF of variable R_0.

Even if the variable R_0 is assumed to follow a particular type of a parametric distribution (e.g. normal), the unconditional density after the integration in Eq. (30) is non-parametric, so the resultant probability distribution is not of the same type and cannot be classified as normal. See in Fig. 6(c).

Now all non-probabilistic information has been converted to the corresponding probability distribution, where the uncertainty quantification approach proposed in previous section is applied. Since our goal was not only to calculate the reliability for certain given parameters but to derive an overview picture of the reliability surface of whole rotor/stator contact system, we will further discover the effects of concerned parameters on system reliability by adjusting their distribution (hyper)parameters. The non-linearity characteristics incorporated in the limit state equation will be discussed in detail.

5.2 The effects of rotation speed & friction coefficient on system reliability

To begin with, the clearance is first set as a fixed value as 1.05, while the mean values of probability distributions (given or transformed) of rotation speed and friction coefficient vary. As mentioned, the rotor/stator coupled system is supposed to be reliable if no rubbing occurs. The boundary condition for deterministic scenario is given as

$$\begin{aligned} &\left(R_0^2 - 1\right)\Omega^4 + R_0^2\left(4\zeta^2 - 2\beta\right)\Omega^2 - 4R_0^2\zeta\Omega + R_0^2\beta^2 \geq 0 \\ &\Omega^2\left(\Omega^2 + 4\zeta^2 - 2\right) + \left(1+\beta\right)^2 \\ &+ f_c^2 + \left(\Omega^2 - f_c^2 - 1 - \beta\right)R_0/R = 0 \\ &b_1^2 - b_1 b_2 b_3 + b_0 b_3^2 = 0, \quad b_1 b_3 > 0 \end{aligned} \tag{31}$$

where the coefficients b_0~b_3 are given as

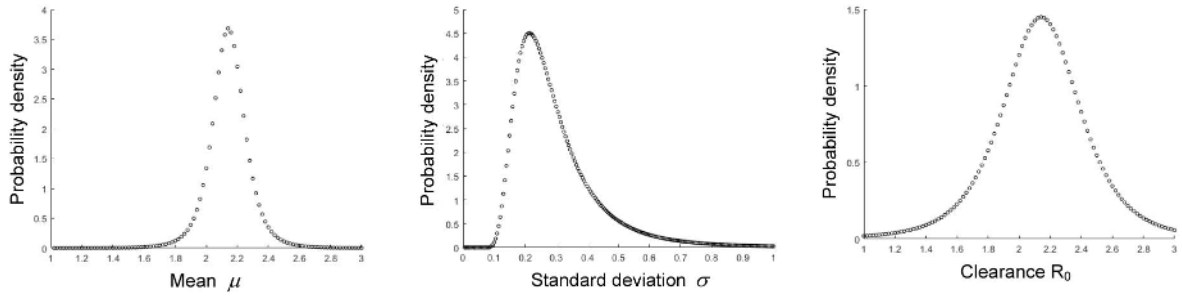

(a) (b) (c)

Fig. 6. (a) PDF of mean μ; (b) PDF of standard deviation σ; (c) unconditional PDF of R_0.

$$b_3 = 4\zeta$$
$$b_2 = 4\zeta^2 + 2\Omega^2 + 2(1+\beta) - R_0/R$$
$$b_1 = 4\left(f_c\Omega + \zeta + \beta\zeta + \Omega^2\zeta\right) - 2\left(f_c\Omega + \zeta\right)R_0/R$$
$$b_0 = \Omega^2\left(\Omega^2 + 4\zeta^2 - 2\right) + \left(1+\beta\right)^2 + f_c^2 + \left(\Omega^2 - f_c^2 - 1 - \beta\right)R_0/R\,.$$

The first equation of Eq. (31) corresponds to the parameter boundary condition of no-rub synchronous motion, while the other two constraints are boundary conditions induced by saddle node bifurcation and Hopf bifurcation, respectively.

Since it is the parameter space of no-rub solution that of interest, we investigated the safe domain of the rotor/stator system by determining the boundary of each system response. In Fig. 7(a) the parameter space of the no-rub solution (region 1) is separated by the region of annular solution (region 2), which is bounded as the lower limit Ω_l and upper limit Ω_u. When the rotation speed either rises across the lower bound or falls across the upper bound, the deflection exceeds the initial clearance, so the rotor contacts with the stator. Noting that the full annular rub bifurcates into partial rub (region 3) through Hopf bifurcation and the saddle node bifurcation condition gives the boundary between no-rub and full annular rub, the existence region of periodic solution is determined. However, due to the inherent nonlinear nature of the rotor/stator system, there may be a coexistence of multiple system response. For instance, both no-rub solution and full annular rub solution exist in region 1+2. The dry whirl or dry whip will be triggered after the full annular rub of the rotor/stator system loses its stability through Hopf bifurcation; thus no-rub and backward whirling coexists in region 1+3. Taking the parameter uncertainty into consideration, the true safe region for rotor/stator system should be the parameter space where only the no-rub solution is valid. Fig. 7(c) shows the fluctuation of reliability for different parameter combinations in the $\Omega - f_c$ parameter plane. For better presentation, its two-dimensional top view is also depicted in Fig. 7(b), which shows a correspondence with the safe region in deterministic scenario but narrower area.

Fig. 8(a) shows the parameter contour lines and reliability surface of the case that non-dimensional clearance has increased to 2. There is no surprise that the safe region is enlarged due to the increasing of clearance. Regarding the

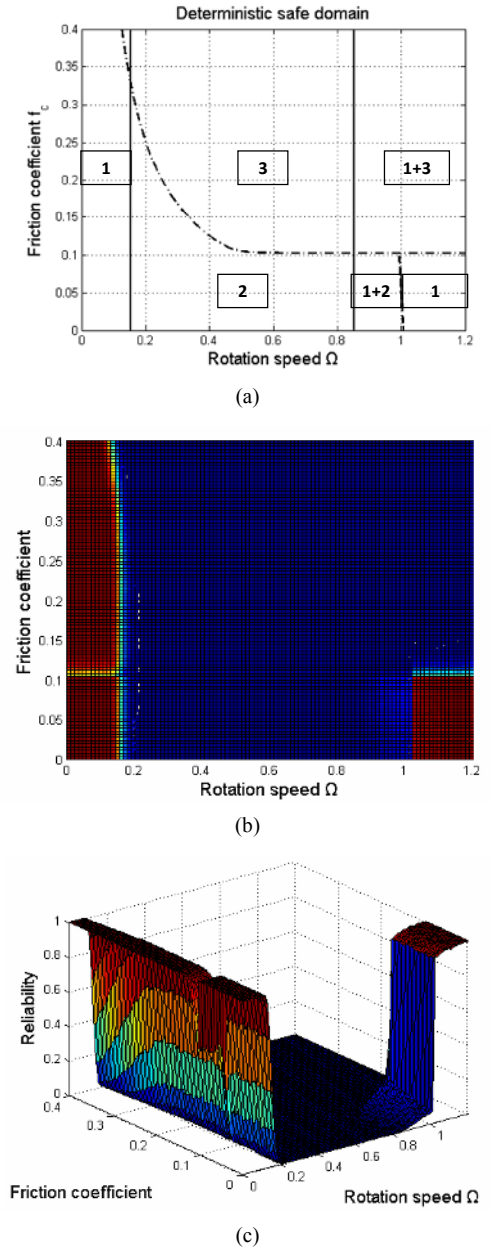

(a)

(b)

(c)

Fig. 7. Safety domain in Ω - f_c parameter plane: (a) In deterministic scenario; (b) with mixed uncertainty; (c) reliability surface ($R_0 = 1.05$).

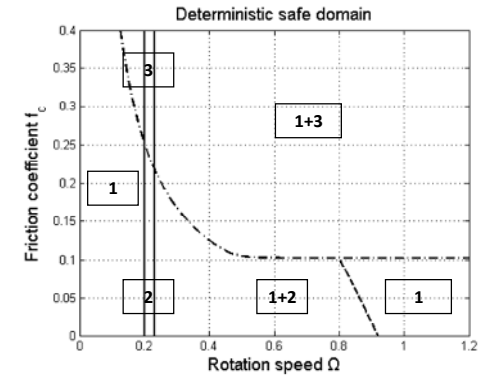

(a)

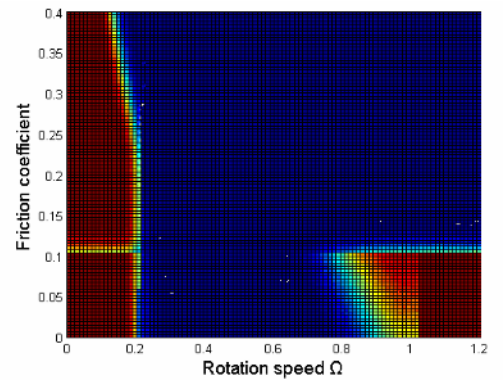

(b)

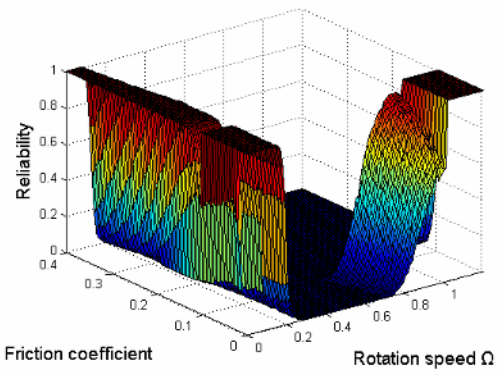

(c)

Fig. 8. Safety domain in Ω - f_c parameter plane: (a) In deterministic scenario; (b) with mixed uncertainty; (c) reliability surface ($R_0 = 2$).

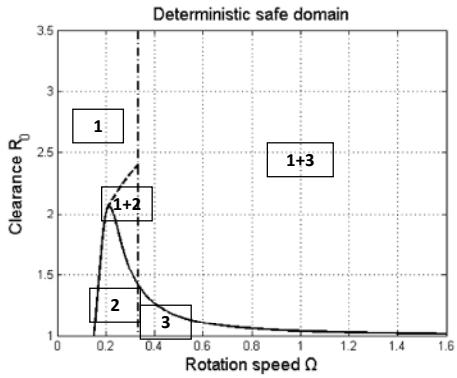

(a)

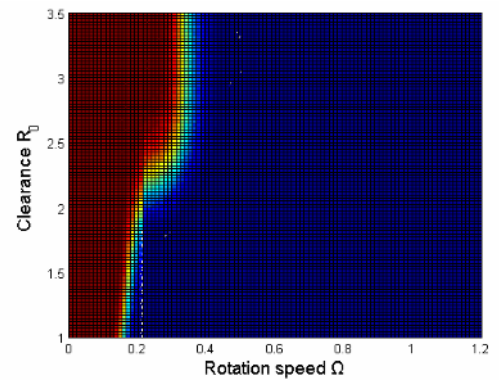

(b)

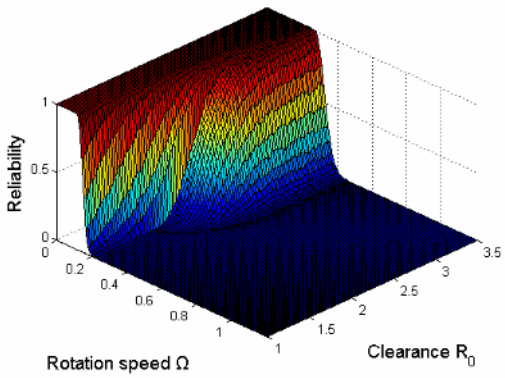

(c)

Fig. 9. Safety domain in Ω - R_0 parameter plane: (a) In deterministic scenario; (b) with mixed uncertainty; (c) reliability surface (friction coefficient $f_c = 0.15$).

shape, the parameter space of full annular rub solution (region 2) significantly shrinks, which is mainly attributed to the change of saddle node bifurcation boundary. The left boundary of the safe region in lower right corner is now determined by the saddle node bifurcation boundary condition (see Fig. 8(b)). The three-dimensional reliability surface for the case of $R_0 = 2$ is also presented in Fig. 8(c).

5.3 The Effects of rotation speed and clearance on system reliability

The influence of rotation speed together with clearance on the system reliability is examined below. To carry out this study, the friction coefficient was first set as 0.15. It is noted that the curve indicating lower bound of full annular rub solation (region 2) interacts with the curve indicating upper bound at the point of R_0 = 2.06, which suggests that there will be no full annular rub solution existing when the clearance is greater than 2.06. Since the synchronous full annular rub bifurcates into partial rub (region 3) through Hopf bifurcation, only the parameter plane on the left side of the vertical dashed line (which stands for the Hopf bifurcation) would possible be the safe region. Virtually, the safe domain in Fig. 9(a) is deter-

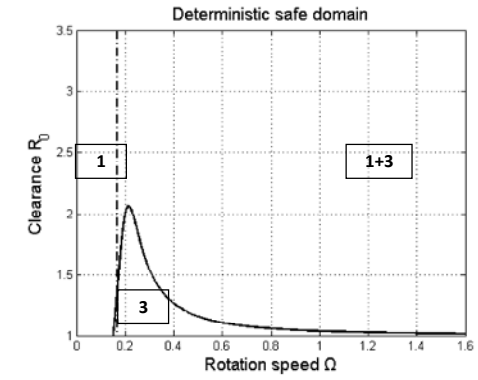

(a)

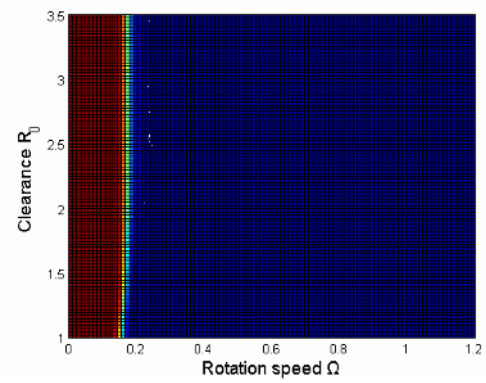

(b)

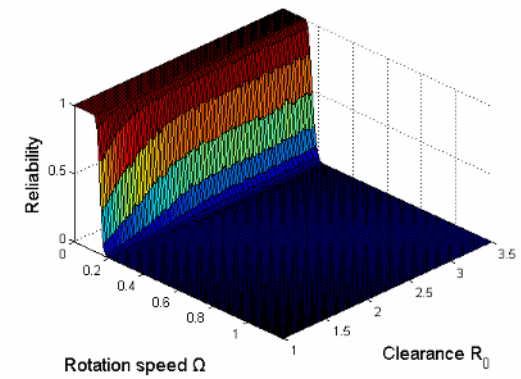

(c)

Fig. 10. Safety domain in Ω - R_0 parameter plane: (a) In deterministic scenario; (b) with mixed uncertainty; (c) reliability surface (friction coefficient $f_c = 0.3$).

mined based on the contributions of linear governing equation condition, saddle node bifurcation condition and the Hopf bifurcation condition together. Fig. 9(b) shows the corresponding safe domain taking uncertainty into account, and the three-dimensional reliability surface is depicted in Fig. 9(c).

To discover the effects of rotation speed and clearance on system reliability for other fixed value of friction coefficient, the contour lines for constraints in Eq. (6) are redrawn for $f_c = 0.3$ in the $\Omega - R_0$ parameter plane in Fig. 10(a). Compared with the case for $f_c = 0.15$, the Hopf bifurcation boundary moves leftward, leading to a narrower safe domain (see in Fig. 10(b)). Since the boundary of no-rub solution and saddle node bifurcation lies outside of the area bounded by the Hopf bifurcation, the safe region is shaped as a rectangle, which is purely determined by the vertical dashed line (Hopf bifurcation) in this scenario (see in Fig. 10(c)).

6. Discussion

The reason for addressing the reliability issue of a Jeffcott rotor is that it serves as the basic model for many practical rotor systems, though it is quite simple compared with many complicated rotor/stator coupled systems. The reliability analysis result has profound significance for new products in the early design and prototyping stage, and also benefits rotary machines already installed in the operation safety. For instance, to meet the reliability requirement, the safe domain derived is quite different with that in a deterministic scenario, which could be a meaningful reference to practical rotors. In the context of uncertain dynamics analysis, the adopted reliability method sufficiently addresses its nonlinear characteristics, namely, the reliability criterion is case-based, in which the physical model is considered. Furthermore, the developed framework deals with mixed aleatory-epistemic uncertainty in a unified way, which is flexible and allows simultaneous processing of probability distribution and interval estimates, indicating successful information aggregation and data fusion. Also, some system responses, such as dry whirl or dry whip, in practice are not considered since they are irrelevant to the reliability of the rotor/stator contact system.

7. Conclusions

The reliability of a typical Jeffcott rotor/stator system subjected to mixed aleatory-epistemic uncertainty was studied. An overall picture of the system global responses was derived analytically. The effects of parameters on reliability were studied incorporating both rotor physical characteristics and inherent uncertain factors. A likelihood-based approach addressing multiple inputs was developed, which enables a comprehensive reliability analysis of the rotor/stator system incorporating all available information (sparse point data, probabilistic distribution and intervals). Some Bayesian techniques were adopted to reduce the computation cost in traditional double loop Monte Carlo method. Since the uncertain factors induced either in manufacturing phase or in assembling stage are inevitable in practical engineering, the developed approach can be applied in industrial manufacturing & mounting, risk assessment, product maintaining etc. and benefits rotary machines from design phase to operation stage.

Acknowledgments

The authors gratefully acknowledge the financial support from the Fundamental Research Funds for the Central Univer-

sities of China under grant FRF-TP-17-056A1 and the China Postdoctoral Science Foundation under Grant 2018M630073.

References

[1] H. F. Black, Interaction of a whirling rotor with a vibrating stator across a clearance annulus, *ARCHIVE International J. of Mechanical Engineering Science,* 10 (1) (1968) 1-12.

[2] W. Zhang, Dynamic instability of multi-degree-of-freedom flexible rotor systems due to full annular rub, *IMechE C*, 252/88 (1988) 305-308.

[3] D. E. Bently, J. J. Yu, P. Goldman and A. Muszynska, Full annular rub in mechanical seals, Part I: Experimental results, *International J. of Rotating Machinery*, 8 (5) (2002) 319-328.

[4] D. E. Bently, P. Goldman and J. J. Yu, Full annular rub in mechanical seals, Part II: Analytical study, *International J. of Rotating Machinery*, 8 (5) (2002) 329-336.

[5] D. W. Childs, Rub-induced parametric excitation in rotors, *J. of Mechanical Design*, 104 (4) (1979) 640-644.

[6] D. W. Childs, Fractional-frequency rotor motion due to nonsymmetric clearance effects, *J. of Engineering for Power*, 104 (3) (1982) 533-541.

[7] F. F. Ehrich, High order subharmonic response of high speed rotors in bearing clearance, *J. of Vibration, Acoustics, Stress, and Reliability in Design,* 110 (1) (1988) 9-16.

[8] Y. B. Kim and S. T. Noah, Quasi-periodic response and stability analysis for a nonlinear Jeffcott rotor, *J. of Sound and Vibration,* 190 (2) (1996) 239-253.

[9] S. K. Choi and S. T. Noah, Mode-locking and chaos in a Jeffcott rotor with bearing clearances, *J. of Applied Mechanics,* 61 (1) (1994) 131-138.

[10] P. Goldman and A. Muszynska, Chaotic behavior of rotor/stator system with rubs, *J. of Engineering for Gas Turbines and Power,* 116 (3) (1994) 692-701.

[11] F. Chu and Z. Zhang, Bifurcation and chaos in a rub-impact Jeffcott rotor system, *J. of Sound and Vibration,* 210 (1) (1998) 1-18.

[12] A. Lingener, Experimental investigation of reverse whirl of a flexible rotor, *Proceedings of 3rd International Conference on Rotor Dynamics* (1990) 13-18.

[13] S. Crandall, From whirl to whip in rotor dynamics, *Proceedings of 3rd International Conference on Rotor dynamics* (1990) 19-26.

[14] A. R. Bartha, Dry friction backward whirl of rotors: Theory, experiments, results, and recommendations, *7th International Symposium on Magnetic Bearings* (2000).

[15] J. Jiang and H. Ulbrich, Stability analysis of sliding whirl in a nonlinear jeffcott rotor with cross-coupling stiffness coefficients, *Nonlinear Dynamics*, 24 (3) (2001) 269-283.

[16] J. Jiang, Determination of the global responses characteristics of a piecewise smooth dynamical system with contact, *Nonlinear Dynamics*, 57 (3) (2009) 351-361.

[17] M. R. Motley and Y. L. Young, Influence of uncertainties on the response and reliability of self-adaptive composite rotors, *Composite Structures*, 94 (1) (2011) 114-120.

[18] J. Didier, J. J. Sinou and B. Faverjon, Study of the nonlinear dynamic response of a rotor system with faults and uncertainties, *J. of Sound and Vibration*, 331 (3) (2012) 671-703.

[19] J. J. Sinou and B. Faverjon, The vibration signature of chordal cracks in a rotor system including uncertainties, *J. of Sound and Vibration*, 331 (1) (2012) 138-154.

[20] H. Liao, Global resonance optimization analysis of nonlinear mechanical systems: Application to the uncertainty quantification problems in rotor dynamics, *Communications in Nonlinear Science and Numerical Simulation*, 19 (9) (2014) 3323-3345.

[21] L. C. Yang, J. G. Zhang, Y. Guo and P. D. Wang, A Bayesian-based reliability estimation approach for corrosion fatigue crack growth utilizing the random walk, *Quality and Reliability Engineering International*, 32 (7) (2016) 2519-2535.

[22] J. Lim, B. Lee and I. Lee, Sequential optimization and reliability assessment based on dimension reduction method for accurate and efficient reliability-based design optimization, *J. of Mechanical Science and Technology*, 29 (4) (2015) 1349-1354.

[23] Y. K. Son and T. Kwon, Storage reliability estimation of one-shot systems using accelerated destructive degradation data, *J. of Mechanical Science and Technology*, 30 (10) (2016) 4439-4442.

[24] F. A. Lara-Molina, E. H. Koroishi and V. Steffen Jr., Uncertainty analysis of flexible rotors considering fuzzy parameters and fuzzy-random parameters, *Latin American J. of Solids and Structures,* 12 (10) (2015) 1807-1823.

[25] S. S. Rao and Y. Qiu, A fuzzy approach for the analysis of rotor-bearing systems with uncertainties, *ASME 2011 International Design Engineering Technical Conferences and Computers and Information in Engineering Conference* (2011) 1033-1044.

[26] M. H. Xu and Z. P. Qiu, A collocation reliability analysis method for probabilistic and fuzzy mixed variables, *Science China Physics*, *Mechanics & Astronomy*, 57 (7) (2014) 1318-1330.

[27] C. Wang, Z. Qiu and Y. He, Fuzzy interval perturbation method for uncertain heat conduction problem with interval and fuzzy parameters, *International J. for Numerical Methods in Engineering*, 104 (5) (2015) 330-346.

[28] K. Zaman et al., A probabilistic approach for representation of interval uncertainty, *Reliability Engineering and System Safety*, 96 (1) (2011) 117-130.

[29] S. Sankararaman and S. Mahadevan, Likelihood-based representation of epistemic uncertainty due to sparse point data and/or interval data, *Reliability Engineering and System Safety*, 96 (7) (2011) 814-824.

[30] D. Wu et al., Probabilistic interval stability assessment for structures with mixed uncertainty, *Structural Safety*, 58 (2016) 105-118.

[31] Y. Zhang, B. Wen and Y. T. Leung Andrew, Reliability analysis for rotor rubbing, *J. of Vibration and Acoustics*, 124

(1) (2002) 58-62.
[32] Y. M. Zhang, B. C. Wen and Q. L. Liu, Reliability sensitivity for rotor-stator systems with rubbing, *J. of Sound and Vibration*, 259 (5) (2003) 1095-1107.
[33] J. P. Spagnol, H. Wu and K. Xiao, Dynamic response of a cracked rotor with an unbalance influenced breathing mechanism, *J. of Mechanical Science and Technology*, 32 (1) (2018) 57-68.
[34] Y. Du, W. Tan and M. Zhou, Time compatibility analysis of web service composition: A modular approach based on petri nets, *IEEE Transactions on Automation Science and Engineering*, 11 (2) (2014) 594-606.
[35] L. Yang, J. Zhang and Y. Guo, Uncertainty representation and quantification for a nonlinear rotor/stator system with mixed uncertainties, *J. of Vibroengineering*, 18 (7) (2016) 4836-4851.
[36] J. C. Helton, Quantification of margins and uncertainties: Conceptual and computational basis, *Reliability Engineering and System Safety,* 96 (9) (2011) 976-1013.
[37] J. C. Helton, Quantification of margins and uncertainties: Alternative representations of epistemic uncertainty, *Reliability Engineering and System Safety*, 96 (9) (2011) 1034-1052.
[38] G. A. Barnard, G. M. Jenkins and C. B. Winsten, Likelihood inference and time series, *J. of the Royal Statistical Society*, *Series A* (1962) 321-372.

Lechang Yang is a post-doctoral in the School of Mechanical Engineering, University of Science and Technology Beijing. He received a Ph.D. from the School of Reliability and Systems Engineering, Beihang University. He also earned a B.S. degree in the school of Aeronautic Science and Engineering, Beihang University. His research is primarily focused on statistics modeling, Bayesian analysis and reliability of nonlinear systems.

Ketai He is an Associate Professor of Mechanical Engineering, University of Science and Technology Beijing. He received his Ph.D. and M.S. in the School of Mechanical Engineering & Automation, Beihang University. His B.S. is from the School of Mechanical Engineering, Shandong University of Technology. His research is primarily focused on quality control and intelligent manufacturing.

Yanling Guo is an experimentalist in the School of Automation Science and Electrical Engineering, Beihang University. She received the M.S. in the School of Automation Science and Electrical Engineering, Beihang University. Her B.S. in Electrical Engineering, Yanshan University. Her research is primarily focused on complex networks and systems, stability theory and nonlinear control.